J. A. Blume
Division of Engineering,
Brown University,
Providence, RI 02912
Assoc. Mem. ASME

Finite, Dynamic Motions of Thin Rate-Dependent Sheets

The transient response of a thin sheet comprised of a rate-dependent solid is determined. The material is assumed to be incompressible, and the constitutive response is governed by a nonlinearly viscous power-law model. The sheet has axially symmetry, but an otherwise arbitrarily varying thickness. Axially symmetric, finite, dynamic motions of the sheet are identified.

Introduction

In this paper, the finite, transient response of an axially symmetric, thin sheet comprised of a rate-dependent, incompressible solid is determined. A Lagrangian formulation, coupled with a theory of generalized plane stress, is employed. The dependence of the motion on the initial thickness profile of the sheet is explored.

Because of its importance in connection with sheet metal forming, plane-stress motions in plastically deforming materials have been the subject of extensive research activity. The prediction of necking in such sheets is a main objective, and several studies, including those by Stören and Rice (1975), Needleman (1976), and Rice (1976), have been carried out using plane-stress approximative assumptions. Needleman and Tvergaard (1977), and Hutchinson, Neale, and Needleman (1978) did studies in both three-dimensional and plane-stress settings, and discuss the validity of the plane-stress theory. Dynamic instabilities of plastically deforming solids were considered by Taylor, Harlow, and Ainsden (1978).

In this paper, a simple material model is used to describe the dynamic response of finitely-deforming, rate-dependent sheets. In uniaxial tension, the Cauchy stress τ is proportional to the rate of strain raised to a power. Using generalized plane stress, axially symmetric motions of a sheet of arbitrary undeformed cross-section are analytically determined.

1 Notation Preliminaries on Finite Deformations of Rate-Dependent Solids

Throughout this paper, lower case and capital letters in boldface designate vectors and (second-order) tensors, respectively. The same letter in lightface appearing with one or more subscripts will signify the appropriate components of the vector or tensor in either cylindrical or Cartesian coordinates.

If $\mathcal{R}$ is the region in three-space occupied by a solid in its reference configuration, a motion is a mapping $\hat{\mathbf{y}}$ described by

$$\mathbf{y}=\hat{\mathbf{y}}(\mathbf{x},t)=\mathbf{x}+\mathbf{u}(\mathbf{x},t) \text{ on } \mathcal{R},\ (t>0), \tag{1}$$

where $\mathbf{x}$ is the position vector of a material point in $\mathcal{R}$, $\hat{\mathbf{y}}(\mathbf{x},t)$ is the position vector of its deformation image at time t, and $\mathbf{u}$ is the associated displacement field. The region occupied by the body at time t will be called $\mathcal{R}_t$, and at each t, the mapping from $\mathcal{R}$ to $\mathcal{R}_t$ is assumed to be one-to-one. The motion $\hat{\mathbf{y}}$ of $\mathcal{R}$ is taken to be twice jointly continuously differentiable with respect to position and time.

This work is concerned with motions of an *incompressible* solid, which can sustain only locally volume-preserving deformations. The mapping (equation) (1) is locally-volume preserving if and only if

$$J\equiv \det \mathbf{F}=1,\ \mathbf{F}=\nabla\hat{\mathbf{y}}. \tag{2}$$

Here, $\mathbf{F}$ is the deformation gradient tensor and J is the Jacobian.

The letter $\mathbf{D}$ denotes the rate-of-deformation tensor, so that

$$\mathbf{D}(\mathbf{y},t)=\operatorname{sym}\nabla\mathbf{v}(\mathbf{y},t) \text{ on } \mathcal{R}_t,\ t>0, \tag{3}$$

in which $\mathbf{v}$ is the Eulerian velocity field:

$$\mathbf{v}(\mathbf{y},t)=\dot{\hat{\mathbf{y}}}(\hat{\mathbf{x}}(\mathbf{y},t),t) \text{ on } \mathcal{R}_t,\ t>0. \tag{4}$$

Here the dot denotes the derivative with respect to time ($\mathbf{x}$ fixed), and $\hat{\mathbf{x}}(\mathbf{y},t)$ is the inverse of $\hat{\mathbf{y}}(\mathbf{x},t)$ at time t: $\hat{\mathbf{x}}(\hat{\mathbf{y}}(\mathbf{x},t),t)=\mathbf{x}$ for all $\mathbf{x}$ in $\mathcal{R}$. The rate of deformation tensor is thus expressible as

$$\mathbf{D}(\hat{\mathbf{y}}(\mathbf{x},t),t)=\frac{1}{2}\{\dot{\mathbf{F}}(\mathbf{x},t)\mathbf{F}^{-1}(\mathbf{x},t)+\mathbf{F}^{-T}(\mathbf{x},t)\dot{\mathbf{F}}^{T}(\mathbf{x},t)\}. \tag{5}$$[1]

This, together with the constraint of local volume-preservation (2) can be found to imply that

$$\operatorname{trace}\mathbf{D}=0 \text{ on } \mathcal{R}_t,\ t>0. \tag{6}$$

If $\boldsymbol{\sigma}$ is the Piola stress tensor accompanying the motion (1), the equations of motion, in absence of body forces, demand that

$$\operatorname{div}\boldsymbol{\sigma}=\rho\ddot{\mathbf{y}},\ \boldsymbol{\sigma}\mathbf{F}^{T}=\mathbf{F}\boldsymbol{\sigma}^{T} \text{ on } \mathcal{R}, \tag{7}$$

with ρ designating the reference mass density. The mass density for the solid at hand is assumed to be constant. The

Contributed by the Applied Mechanics Division of THE AMERICAN SOCIETY OF MECHANICAL ENGINEERS for publication in the JOURNAL OF APPLIED MECHANICS.

Discussion on this paper should be addressed to the Technical Editor, Leon M. Keer, the Technological Institute, Northwestern University, Evanston, IL 60208, and will be accepted until two months after final publication of the paper itself in the JOURNAL OF APPLIED MECHANICS. Manuscript received and accepted by the ASME Applied Mechanics Division, June 12, 1989.

[1] If $\mathbf{F}^{T}$ stands for the transpose of $\mathbf{F}$, while $\mathbf{F}^{-1}$ is its inverse and $\mathbf{F}^{-T}$ denotes the transposed inverse of $\mathbf{F}$.

Eulerian version of equation (7) may be written in terms of the Cauchy stress field τ, which is linked to the Piola stress tensor through

$$\tau(\mathbf{y},t)=\sigma(\mathbf{x},t)\mathbf{F}^T(\mathbf{x},t),\ \mathbf{y}=\hat{\mathbf{y}}(\mathbf{x},t). \tag{8}$$

The equations of motion are alternately cast as

$$\operatorname{div}\tau(\mathbf{y},t)=\rho\left\{\frac{\partial}{\partial t}\mathbf{v}(\mathbf{y},t)+[\nabla\mathbf{v}(\mathbf{y},t)]\mathbf{v}(\mathbf{y},t)\right\},$$

$$\tau(\mathbf{y},t)=\tau^T(\mathbf{y},t)\ \text{for all}\ \mathbf{y}\in\mathcal{R}_t, \tag{9}$$

with $\mathbf{v}$ again signifying the Eulerian velocity field. In arriving at the above, the local volume preservation of the motion and the conservation of mass postulate have been used in writing ρ for the current mass density.

The stress response of the materials at hand is assumed to be well described by a purely rate-dependent, power-law type constitutive model. In particular, if ν and γ are material constants with $\nu>0$ and $\gamma>-1$, then

$$\tau=-p\mathbf{1}+\nu d^{\gamma}\mathbf{D}\ \text{on}\ \mathcal{R}_t, \tag{10}$$

where p is the pressure field which accommodates the constraint of incompressibility, $\mathbf{1}$ is the identity tensor, and

$$d=|\mathbf{D}|=\sqrt{D_{ij}D_{ij}}\ \text{on}\ \mathcal{R}_t. \tag{11}$$

Note that the second of equation (9) is satisfied automatically. Although the parameter γ is dimensionless, the constant ν has the peculiar units of time raised to the power $(\gamma-1)$, multiplied by mass/length. Typically, for describing the behavior of metals at very high strain rates, γ is close to -1.

On account of equations (8) and (5), the Piola stress for such materials may be written as

$$\sigma=-p\mathbf{F}^{-T}+\frac{1}{2}\nu d^{\gamma}\{\dot{\mathbf{F}}\mathbf{C}^{-1}-(\mathbf{F}^{-T})^{\cdot}\}\ \text{on}\ \mathcal{R},\ \mathbf{C}=\mathbf{F}^T\mathbf{F}. \tag{12}$$

It is convenient to express the equations of motion in dimensionless form. To this end, if l and v are, respectively, a characteristic length and velocity of a given boundary value problem, one defines dimensionless independent variables $\bar{\mathbf{x}}$ and $\bar{t}$ through

$$\bar{\mathbf{x}}=\mathbf{x}/l,\ \bar{t}=\frac{tv}{l}, \tag{13}$$

and dimensionless dependent variables $\bar{\mathbf{y}}$, $\bar{\sigma}$, and $\bar{p}$, by

$$\bar{\mathbf{y}}(\bar{\mathbf{x}},\bar{t})=\frac{1}{l}\mathbf{y}(\bar{\mathbf{x}}l,\bar{t}l/v),\ \bar{\sigma}(\bar{\mathbf{x}},\bar{t})=\frac{1}{v^2\rho}\sigma(\bar{\mathbf{x}}l,\bar{t}l/v),$$

$$\bar{p}(\bar{\mathbf{x}},\bar{t})=\frac{1}{v^2\rho}p(\bar{\mathbf{x}}l,\bar{t}l/v). \tag{14}$$

The constitutive law (12) may thus be written in dimensionless form as

$$\bar{\sigma}=-\bar{p}\bar{\mathbf{F}}^{-T}+\frac{1}{2}\bar{\nu}\bar{d}^{\gamma}\{\dot{\bar{\mathbf{F}}}\bar{\mathbf{C}}^{-1}-(\bar{\mathbf{F}}^{-T})^{\cdot}\}\ \text{on}\ \mathcal{R},\ \bar{\mathbf{C}}=\bar{\mathbf{F}}^T\bar{\mathbf{F}}. \tag{15}$$

Here, the dot denotes differentiation with respect to $\bar{t}$,

$$\bar{\mathbf{F}}=\nabla_{\bar{\mathbf{x}}}\bar{\mathbf{y}},\ \bar{d}=\frac{1}{2}|\dot{\bar{\mathbf{F}}}(\mathbf{x},t)\bar{\mathbf{F}}^{-1}(\mathbf{x},t)+\bar{\mathbf{F}}^{-T}(\mathbf{x},t)\dot{\bar{\mathbf{F}}}^T(\mathbf{x},t)|, \tag{16}$$

and $\bar{\nu}$ is a dimensionless viscosity-like material parameter, given by

$$\bar{\nu}=\frac{\nu v^{\gamma-1}}{\rho l^{\gamma+1}}. \tag{17}$$

When $\gamma=0$, so that the constitutive law at hand describes a Newtonian fluid, $1/\bar{\nu}$ is the standard Reynolds number. The equations of motion (7), become

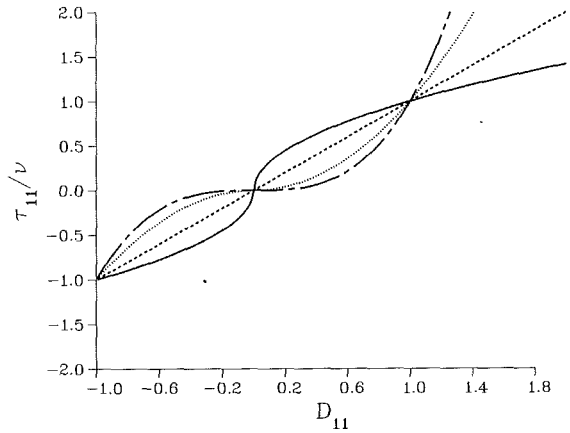

Fig. 1 Response of the power-law viscous solids in uniaxial stress; $\gamma=-.9$: solid line, $\gamma=0$: dashed line, $\gamma=1$: dotted line, $\gamma=2$: broken dashed line

$$\operatorname{div}_{\bar{\mathbf{x}}}\bar{\sigma}=\ddot{\bar{\mathbf{y}}},\ \bar{\sigma}\bar{\mathbf{F}}^T=\bar{\mathbf{F}}\bar{\sigma}^T\ \text{on}\ \mathcal{R}. \tag{18}$$

In addition, if $\bar{\tau}$ is a dimensionless Cauchy stress tensor, then one has from equation (8)

$$\bar{\tau}(\bar{\mathbf{y}},\bar{t})\equiv\frac{1}{v^2\rho}\tau(\bar{\mathbf{y}}l,\bar{t}l/v)=\sigma(\bar{\mathbf{x}},\bar{t})\bar{\mathbf{F}}^T(\bar{\mathbf{x}},\bar{t}). \tag{19}$$

In the analyses that follow, the nondimensional variables introduced previously will be used, and to avoid cumbersome notation, ν, $\mathbf{x}$, t, $\hat{\mathbf{y}}$, σ, p, and τ will be written in place of $\bar{\nu}$, $\bar{\mathbf{x}}$, $\bar{t}$, $\bar{\mathbf{y}}$, $\bar{\sigma}$, $\bar{p}$, and $\bar{\tau}$, with the understanding that the former now refer to the associated *dimensionless* quantities.

In order to understand the behavior of the material model, consider a state of *uniaxial stress*. In this case, only one stress component, say τ_{11}, is nonzero; all others vanish identically. One motion and pressure field which corresponds to such a state is

$$\hat{y}_1(\mathbf{x},t)=\lambda(t)x_1,\ \hat{y}_2(\mathbf{x},t)=\lambda^{-1/2}(t)x_2,\ \hat{y}_3(\mathbf{x},t)=\lambda^{-1/2}(t)x_3,$$

$$p(\mathbf{x},t)=-\frac{1}{2}\nu\left(\frac{3}{2}\right)^{\gamma/2}\left|\frac{\dot{\lambda}}{\lambda}\right|^{\gamma}\frac{\dot{\lambda}}{\lambda}. \tag{20}$$

Here, $\lambda>0$ for $t>0$, and λ is a twice continuously differentiable function of time. The associated spatial velocity field has the components

$$v_1(\mathbf{y},t)=\frac{\dot{\lambda}(t)}{\lambda(t)}y_1,\ v_2(\mathbf{y},t)=-\frac{1}{2}\frac{\dot{\lambda}(t)}{\lambda(t)}y_2,$$

$$v_3(\mathbf{y},t)=-\frac{1}{2}\frac{\dot{\lambda}(t)}{\lambda(t)}y_3, \tag{21}$$

and only the on-diagonal components of the rate-of-deformation tensor $\mathbf{D}$ are nonzero:

$$D_{11}=\frac{\dot{\lambda}(t)}{\lambda(t)},\ D_{22}=D_{33}=-\frac{1}{2}D_{11}. \tag{22}$$

One has

$$\tau_{11}=\bar{\nu}\frac{\dot{\lambda}}{\lambda}\left|\frac{\dot{\lambda}}{\lambda}\right|^{\gamma}\equiv\bar{\nu}D_{11}|D_{11}|^{\gamma},\ \bar{\nu}=\nu\left(\frac{3}{2}\right)^{\gamma/2+1}. \tag{23}$$

Plots of D_{11} versus τ_{11} are given in Fig. 1.

2 Problem Formulation

If (r,θ,z) are cylindrical coordinates of the point with position $\mathbf{x}$ in Euclidean three-space, the solid initially occupies the disk-shaped region $\mathcal{R}$, described by

$$\mathcal{R}=\{\mathbf{x}\,|-h(r)<z<h(r),\ 0\le r\le 1,\ 0\le\theta<2\pi\}. \tag{24}$$

Here, $h(r)$ is a continuously differentiable, positive-valued

function of the in-plane radius r. Note that the normalizing dimension of the problem is taken as the disk radius. We assume that

$$h(r) \ll 1, \quad \left|\frac{dh}{dr}\right| \ll 1, \; 0 \le r \le 1, \tag{25}$$

so that the disk is thin and the function $h(r)$ is *slowly varying*.

The faces of the plate, $z = \pm h(r)$, are traction-free while the edge, $r = 1$, is subjected to a time-dependent radial pressure with magnitude $f(t)$. If $\mathbf{n}$ is the outer unit normal vector to the boundary of $\mathcal{R}$, the nominal stress therefore obeys

$$\boldsymbol{\sigma}\mathbf{n} = \mathbf{0} \text{ on } z = \pm h(r), \; \boldsymbol{\sigma}\mathbf{n} = f\mathbf{n} \text{ on } r = 1. \tag{26}$$

The cylindrical components of $\mathbf{n}$ on the faces of the disk are

$$n_r = \frac{h'(r)}{\sqrt{1+[h'(r)]^2}}, \; n_\theta = 0,$$
$$n_z = \pm \frac{1}{\sqrt{1+[h'(r)]^2}}, \; h'(r) \equiv \frac{dh}{dr}(r), \tag{27}$$

where the plus or minus sign holds according as $\mathbf{n}$ is the outer unit normal vector to the upper or lower face of $\mathcal{R}$. Using equations (27) and (26), one finds that the nominal stress components conform to

$$\begin{aligned} &\pm\sigma_{rr}(r,z,t)h'(r) - \sigma_{rz}(r,z,t) = 0, \\ &\pm\sigma_{\theta r}(r,z,t)h'(r) - \sigma_{\theta z}(r,z,t) = 0, \\ &\pm\sigma_{zr}(r,z,t)h'(r) - \sigma_{zz}(r,z,t) = 0, \text{ on } z = \pm h(r), \; (0 \le r \le 1). \end{aligned} \tag{28}$$

Since $\mathbf{n}$ has components $n_r = 1$, $n_\theta = n_z = 0$ on the disk edge, the second of equation (26) demands that

$$\begin{aligned} &\sigma_{rr}(1,z,t) = f(t), \; \sigma_{\theta r}(1,z,t) = \sigma_{zr}(1,z,t) = 0 \\ &\qquad -h(1) \le z \le h(1), \; t > 0. \end{aligned} \tag{29}$$

Initially, the disk is undeformed, so that any motion $\hat{\mathbf{y}}$ of $\mathcal{R}$ must obey

$$\begin{aligned} &\hat{\mathbf{y}}(\mathbf{x},t) = \mathbf{x} \text{ for all } \mathbf{x} \in \mathcal{R}, \text{ or} \\ &\hat{R}(r,z,t) = r, \; \hat{Z}(r,z,t) = z \text{ at } t = 0, -h(r) \le z \le h(r), \; 0 \le r \le 1. \end{aligned} \tag{30}$$

Here, $\hat{R} = \hat{R}(r,z,t)$ is the radial component of $\hat{\mathbf{y}}$, while $\hat{Z} = \hat{Z}(r,z,t)$ is the component of $\hat{\mathbf{y}}$ in the z-direction. Although $\hat{R} = 0$ when $r = 0$ and $\hat{Z} = 0$ when $z = 0$, $\hat{R}$ and $\hat{Z}$ are otherwise nonvanishing and suitably smooth.

The symmetries inherent in the problem give

$$\begin{aligned} &\hat{R}(r,z,t) = \hat{R}(r,-z,t), \; \hat{Z}(r,z,t) = -\hat{Z}(r,-z,t), \\ &\qquad -h(r) < z < h(r), \; r > 0, \end{aligned} \tag{31}$$

as well as

$$\begin{aligned} &\sigma_{rr}(r,z,t) = \sigma_{rr}(r,-z,t), \\ &\sigma_{\theta\theta}(r,z,t) = \sigma_{\theta\theta}(r,-z,t), \; \sigma_{zz}(r,z,t) = \sigma_{zz}(r,-z,t), \\ &\sigma_{rz}(r,z,t) = -\sigma_{rz}(r,-z,t), \; \sigma_{zr}(r,z,t) = -\sigma_{zr}(r,-z,t); \end{aligned} \tag{32}$$

all other stress components vanish. The second of (28) is thus automatically satisfied, as are the the last of (29).

At this point, it is useful to recall that for axially symmetric motions, the component versions of the balance of linear momentum equations in the first of (18) reduce to

$$\begin{aligned} &\frac{\partial}{\partial r}\sigma_{rr} + \frac{1}{r}(\sigma_{rr} - \sigma_{\theta\theta}) + \frac{\partial}{\partial z}\sigma_{rz} = \frac{\partial^2 \hat{R}}{\partial t^2}, \\ &\frac{\partial}{\partial r}\sigma_{zr} + \frac{\partial}{\partial z}\sigma_{zz} + \frac{1}{r}\sigma_{zr} = \frac{\partial^2 \hat{Z}}{\partial t^2}. \end{aligned} \tag{33}$$

Using plane-stress approximative assumptions, motions of the plate that are axially symmetric as well as symmetric about the plane $z = 0$ will be calculated. Let Π stand for the midplane ($z = 0$) of $\mathcal{R}$, and if g is a function defined on $\mathcal{R}$, $\mathring{g}$ will be used to denote its restriction to Π. The aim of the following is to characterize the deformation parameter $\mathring{R}$, along with the stress components $\mathring{\sigma}_{rr}$ amd $\mathring{\sigma}_{\theta\theta}$ by assuming that the thickness averages of the in-plane stress components are well approximated by their midplane values, and that the midplane value of the out-of-plane stress component, σ_{zz} is approximately zero. Thus, it is assumed that

$$\begin{aligned} &\mathring{\sigma}_{zz} \approx 0, \; \frac{1}{2h(r)}\int_{-h(r)}^{h(r)} \sigma_{rr}(r,z,t)\,dz \approx \mathring{\sigma}_{rr}(r,t), \\ &\frac{1}{2h(r)}\int_{-h(r)}^{h(r)} \sigma_{\theta\theta}(r,z,t)\,dz \approx \mathring{\sigma}_{\theta\theta}(r,t) \text{ on } \Pi. \end{aligned} \tag{34}$$

The motivation for these assumptions comes from (25), the third of (28), and the second of (33).

Integrating the first of the equations of motion equation (33) through the thickness of $\mathcal{R}$ leads to

$$\int_{-h(r)}^{h(r)} \left\{\frac{\partial}{\partial r}\sigma_{rr} + \frac{1}{r}(\sigma_{rr} - \sigma_{\theta\theta}) - \frac{\partial^2 \hat{R}}{\partial t^2}\right\} dz + \sigma_{rz}\Big|_{z=-h(r)}^{z=h(r)} = 0. \tag{35}$$

The first of (28) and the assumptions of (34) enable

$$\frac{\partial}{\partial r}\mathring{\sigma}_{rr} + + \frac{1}{r}(\mathring{\sigma}_{rr} - \mathring{\sigma}_{\theta\theta}) + \frac{h'}{h}\mathring{\sigma}_{rr} = \frac{\partial^2 \mathring{R}}{\partial t^2} \text{ on } \Pi. \tag{36}$$

With a view towards expressing the stresses $\mathring{\sigma}_{rr}$ and $\mathring{\sigma}_{\theta\theta}$ in terms of the deformation parameter $\mathring{R}$, note that equation (31) implies that the nonzero cylindrical components of the midplane deformation gradient tensor $\mathring{\mathbf{F}}$ are

$$\mathring{F}_{rr} = \mathring{R}_{,r}, \; \mathring{F}_{\theta\theta} = \mathring{R}/r, \; \mathring{F}_{zz} = \mathring{\lambda} \equiv \partial\hat{Z}(r,0,t)/\partial z \text{ on } \Pi. \tag{37}$$

Here, $\mathring{\lambda}$ is the midplane value of the out-of-plane stretch, $\partial\mathring{R}/\partial r \equiv \mathring{R}_{,r}$, and $\partial\mathring{R}/\partial t \equiv \mathring{R}_{,t}$. Incompressibility demands that $\det \mathring{\mathbf{F}} = 1$ on Π, whence

$$\mathring{\lambda} = \frac{r}{\mathring{R}_{,r}\mathring{R}} \text{ on } \Pi. \tag{38}$$

Therefore, $\mathring{\lambda}$ is fully determined by the function $\mathring{R}(r,t)$.

The stress components are now found on Π from (15) as

$$\begin{aligned} &\mathring{\sigma}_{rr} = \left\{-\mathring{p} + \nu d^\gamma \frac{\mathring{R}_{,rt}}{\mathring{R}_{,r}}\right\}\frac{1}{\mathring{R}_{,r}}, \; \mathring{\sigma}_{\theta\theta} = \left\{-\mathring{p} + \nu d^\gamma \frac{\mathring{R}_{,t}}{\mathring{R}}\right\}\frac{r}{\mathring{R}}, \\ &\mathring{\sigma}_{33} = \left\{-\mathring{p} - \nu d^\gamma\left[\frac{\mathring{R}_{,t}}{\mathring{R}} + \frac{\mathring{R}_{,rt}}{\mathring{R}_{,r}}\right]\right\}\frac{\mathring{R}\mathring{R}_{,r}}{r}, \end{aligned} \tag{39}$$

and

$$d = \sqrt{2\left[\left(\frac{\mathring{R}_{,rt}}{\mathring{R}_{,r}}\right)^2 + \left(\frac{\mathring{R}_{,t}}{\mathring{R}}\right)^2 + \frac{\mathring{R}_{,rt}\mathring{R}_{,t}}{\mathring{R}_{,r}\mathring{R}}\right]} \text{ on } \Pi. \tag{40}$$

The last of (39), in conjunction with the plane-stress assumption appearing in the first of (34) enables one to express the midplane pressure field $\mathring{p}$ as

$$\mathring{p} = -\nu d^\gamma\left[\frac{\mathring{R}_{,t}}{\mathring{R}} + \frac{\mathring{R}_{,rt}}{\mathring{R}_{,r}}\right] \text{ on } \Pi, \tag{41}$$

whence,

$$\begin{aligned} &\mathring{\sigma}_{rr} = \nu d^\gamma\left[\frac{\mathring{R}_{,t}}{\mathring{R}} + 2\frac{\mathring{R}_{,rt}}{\mathring{R}_{,r}}\right]\frac{1}{\mathring{R}_{,r}}, \\ &\mathring{\sigma}_{\theta\theta} = \nu d^\gamma\left[2\frac{\mathring{R}_{,t}}{\mathring{R}} + \frac{\mathring{R}_{,rt}}{\mathring{R}_{,r}}\right]\frac{r}{\mathring{R}}. \end{aligned} \tag{42}$$

On entering (40) and (42) into (36), one is led to a nonlinear, partial differential equation of motion for $\mathring{R}$ with variable coefficients. This equation involves two derivatives of $\mathring{R}$ with respect to r, and two derivatives with respect to time.

In order find solutions to the partial differential equation for $\mathring{R}$, set

$$\mathring{R}(r,t) = A(t)q(r),\ 0 \le r \le 1,\ t > 0, \tag{43}$$

with A and q twice differentiable. Other than the vanishing of q at $r=0$, neither q nor A may have any zeros. It is assumed, without loss of generality, that $A>0$ for $t \ge 0$ and $q>0$ for $0<r\le 1$. The functions A and q will be determined by the equation of motion mentioned previously. Unless one finds that this equation demands $q(r)=r$ for $(0\le r\le 1)$ and $A(t)=1$ at $t=0$, the above separated form for $\mathring{R}$ will be in conflict with the initial condition (30), which demands that the disk be initially undeformed. It will emerge from what follows that for certain choices of the initial disk profile $h(r)$, these initial conditions can be satisfied exactly. For other choices of h, the solutions obtained via the variable separation cannot conform the initial condition, and these results may be interpreted as descriptive of the large-time behavior of the disk.

Combining (43) with (40), one finds

$$d = \sqrt{6}\left|\frac{\dot{A}}{A}\right| \quad \dot{A} \equiv \frac{dA}{dt}. \tag{44}$$

and (42) leads to

$$\mathring{\sigma}_{rr} = \frac{m(t)}{q'(r)},\ \mathring{\sigma}_{\theta\theta} = r\frac{m(t)}{q(r)} \text{ on } \Pi,$$

$$q' \equiv \frac{dq}{dr},\ m = \frac{3\nu 6^{\gamma/2}}{A}\left|\frac{\dot{A}}{A}\right|^{\gamma}\left(\frac{\dot{A}}{A}\right). \tag{45}$$

The above, in conjunction with the first of (29), implies that

$$m(t) = q'(1)f(t),\ t>0. \tag{46}$$

Because A will be determined from the equation of motion, the edge load f required to sustain motions of the form (43) will also be a consequence of the analysis. Owing to the positivity of A and ν, the edge load is tensile or compressive according as the radial velocity $\dot{A}$ is positive or negative.

Substitution from (43) and (45) into the equilibrium equation (36) and rearranging leads to the following pair of ordinary differential equations for q and A:

$$-r[qq'' + (q')^2] + qq' + r\frac{h'}{h}qq' - \alpha r q^2 (q')^2 = 0,\ 0 \le r \le 1, \tag{47}$$

and

$$\ddot{A}A = \beta\left|\frac{\dot{A}}{A}\right|^{\gamma}\left(\frac{\dot{A}}{A}\right),\ \beta = \alpha 3\nu 6^{\gamma/2}. \tag{48}$$

In the above, α is a constant separation parameter. Note that (48) can be written as

$$\frac{d}{dt}\left\{\frac{1}{2}\dot{A}^2\right\} = \beta\left|\frac{\dot{A}}{A}\right|^{\gamma+2}, \tag{49}$$

and since ν is positive by assumption, the radial speed $|\dot{A}|$ of the disk is monotone increasing, decreasing, or is constant, according as the separation parameter α is positive, negative, or zero.

If one sets

$$s(r) = q(r)q'(r),\ 0 \le r \le 1, \tag{50}$$

in the spatial equation (47), then the latter reduces to the first-order Ricatti equation,

$$s' - \left(\frac{1}{r} + \frac{h'}{h}\right)s + \alpha s^2 = 0. \tag{51}$$

The case in which $\alpha = 0$ corresponds to the quasi-static case, since (48) demands that $\ddot{A} = 0$ for all time, and

$$A(t) = c_1 t + c_2 \text{ for all } t>0,\ c_1,\ c_2 \text{ constant}. \tag{52}$$

The solution to (51) when $\alpha = 0$ is given by

$$s(r) = crh(r). \tag{53}$$

Here, c is a constant. Bearing in mind that $\mathring{R}(0,t) = 0$, one finds on integrating equation (50) that

$$q(r) = \sqrt{2c\int_0^r lh(l)dl}. \tag{54}$$

The constant c can be taken as unity without loss of generality. Consequently, one has from (43)

$$\mathring{R}(r,t) = [c_1 t + c_2]\sqrt{2\int_0^r lh(l)dl}. \tag{55}$$

This solution can satisfy the initial condition $\mathring{R}(r,0) = r$ exactly only if the undeformed disk profile is independent of r: $h(r) = h_o = \text{constant}$. If this is not the case, the solution given above might correspond to the large-time behavior of the sheet.

According to (55) and (38), the out-of-plane stretch $\mathring{\lambda}$ is given by

$$\mathring{\lambda}(r,t) = \frac{1}{A^2(t)h(r)}. \tag{56}$$

The boundary $z = h(r)$ is thus approximately mapped to the plane $y_3 = Z = \mathring{\lambda}(r,t)h(r) = A^{-2}(t)$, regardless of the initial thickness profile h. The sheet is transformed into one which is approximately flat.

As far as the stresses are concerned in this quasi-static case, the nominal and Cauchy stresses are found from equations (55), (42), and (8):

$$\mathring{\sigma}_{rr} = m(t)\ \frac{rh(r)}{\sqrt{2\int_0^r lh(l)dl}},\ \mathring{\sigma}_{\theta\theta} = \frac{m(t)r}{\sqrt{2\int_0^r lh(l)dl}},$$

$$\tau_{rr} = \tau_{\theta\theta} = m(t)A(t), \tag{57}$$

with m given by (52) and the last of (45). Note that the Cauchy stresses are constant.

Turning next to the dynamic case, assume that $\alpha \ne 0$. Equation (51) is solved by setting

$$s(r) = \frac{w'(r)}{\alpha w(r)},\ 0 \le r \le 1, \tag{58}$$

with w a nonvanishing, suitably smooth function of r. This substitution reduces equation (51) to

$$w''(r) - \left(\frac{1}{r} + \frac{h'(r)}{h(r)}\right)w'(r) = 0, \tag{59}$$

and one has

$$w(r) = c\int_0^r lh(l)dl + d,\quad c,\ d \text{ constant}, \tag{60}$$

so that (58) and (50) and the fact that $q(0) = 0$ demand

$$q(r) = \sqrt{\frac{2}{\alpha}\ \log\left\{c\int_0^r lh(l)dl + 1\right\}},\ 0 \le r \le 1. \tag{61}$$

In order for equation (61) to be meaningful, $c \ne 0$ and the sign of c must correspond to the sign of α, with

$$c > -\frac{1}{\int_0^1 lh(l)dl}. \tag{62}$$

The initial condition $\mathring{R}(r,0) = A(0)q(r) = r$ for all r between 0 and 1 can be satisfied identically in this case only if

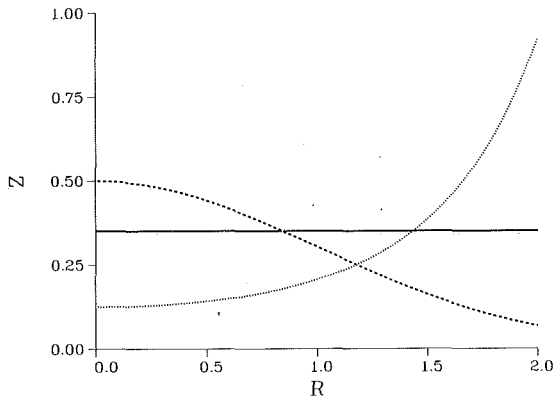

Fig. 2 Disk shapes described by $h(r)=k_1\exp\{k_2r^2\}$; $k_2=0$: solid line, $k_2>0$: dotted line, $k_2<0$, dashed line

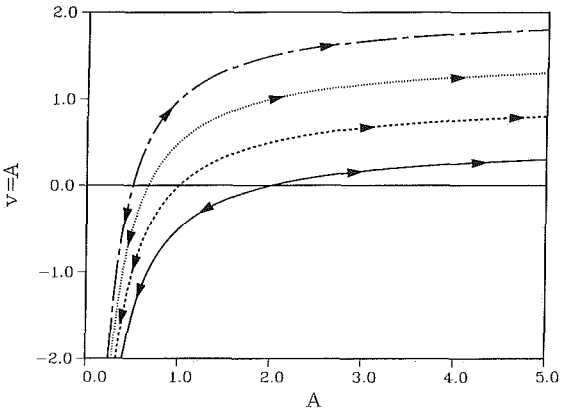

Fig. 3 Phase-plane trajectories for $\gamma=0$ and $\beta=1$

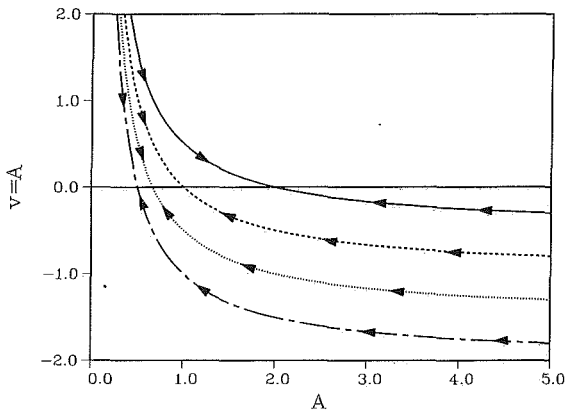

Fig. 4 Phase-plane trajectories for $\gamma=0$ and $\beta=-1$

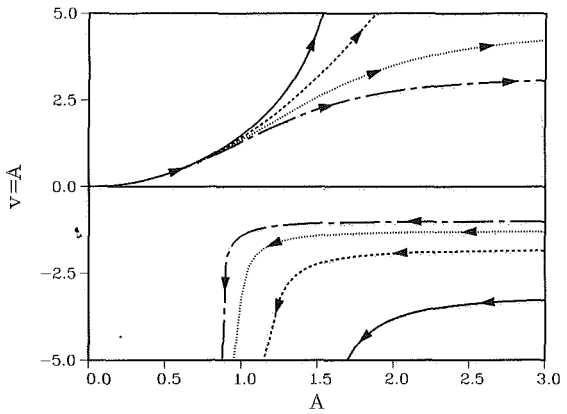

Fig. 5 Phase-plane trajectories for $\gamma=2$ and $\beta=1$

$$h(r)=k_1e^{k_2r^2},\ (0\le r\le 1), \tag{63}$$

in which k_1 and k_2 are constants; $k_1>0$. According as k_2 is positive, negative, or zero, h given above describes one of the shapes shown in Fig. 2. For the disk profile in (63), in order that $\mathring{R}(r,0)=r$, one may choose $A(t)=1$ at $t=0$, and $\alpha=k_2$. If the initial disk thickness profile is *not* given by the above formula, the following results might be interpretable as descriptive of the long-time behavior of the disk.

Solution of the temporal equation (48) in the dynamic case ($\alpha\neq 0$) will be put off until later. For now, note that the out-of-plane stretch $\mathring{\lambda}$ is found from (61), (43), and (38) to conform to

$$\mathring{\lambda}(r,t)=\frac{\alpha}{A^2(t)h(r)}\left[\int_0^r lh(l)dl+\frac{1}{c}\right]. \tag{64}$$

The image of the faces of the sheet, $z=\pm h(r)$, are approximately carried onto the boundary described by

$$Z=\hat{Z}(r,\pm h(r),t)\approx$$
$$\mathring{\lambda}(r,t)h(r)=\pm\frac{\alpha}{A^2(t)}\left[\int_0^r lh(l)dl+\frac{1}{c}\right]. \tag{65}$$

Owing to the fact that $R=\mathring{R}(r,t)=A(t)q(r)$, one has from (61) and (65) the following expression for the thickness Z of the deformed disk as a function of radial distance R at time t:

$$Z=\pm\frac{\alpha}{2cA^2}e^{1/2\alpha R^2/A^2},\ (0\le R\le A(t)q(1)). \tag{66}$$

As in the quasi-static case, the plane-stress approximations predict that the profile of the deformed disk is independent of the initial disk thickness $h(r)$. As was mentioned earlier, A is either monotonically increasing, monotonically decreasing, or is constant. In the case of increasing A, the disk edges will be extended and the disk will be thinned and flattened. If A is decreasing, the disk is thickened as its radius is reduced.

The in-plane stress components are determined with the aid of (45), (61), and (8) as

$$\mathring{\sigma}_{rr}=m(t)\frac{rh(r)}{\alpha q(r)[\int_0^r lh(l)dl+1/c]},\quad \mathring{\sigma}_{\theta\theta}=\frac{m(t)r}{q(r)},$$
$$\tau_{rr}=\tau_{\theta\theta}=m(t)A(t); \tag{67}$$

the Cauchy stresses are again constant.

The autonomous, second-order equation (48) for A admits an implicit solution that is well interpreted with the aid of the phase plane. Bearing in mind that $\gamma>-1$ by assumption, note that equation (48) can be written as

$$\frac{d}{dt}\left\{\dot{A}\,|\dot{A}|^{-\gamma}+\beta\frac{1-\gamma}{1+\gamma}A^{-(1+\gamma)}\right\}=0\ (\gamma\neq 1),$$
$$\frac{d}{dt}\left\{\log|\dot{A}|+\frac{1}{2}\beta A^{-2}\right\}=0\ (\gamma=1). \tag{68}$$

Thus, if

$$v(t)=\dot{A}(t), \tag{69}$$

the phase-plane trajectories of a solution A to (48) are described by the curves

$$v|v|^{\gamma}+\beta\frac{1-\gamma}{1+\gamma}A^{-(1+\gamma)}=d\ (\gamma\neq 1),$$
$$\log|v|+\frac{1}{2}\beta A^{-2}=d\ (\gamma=1) \tag{70}$$

in the (A,v)-plane, with d constant.

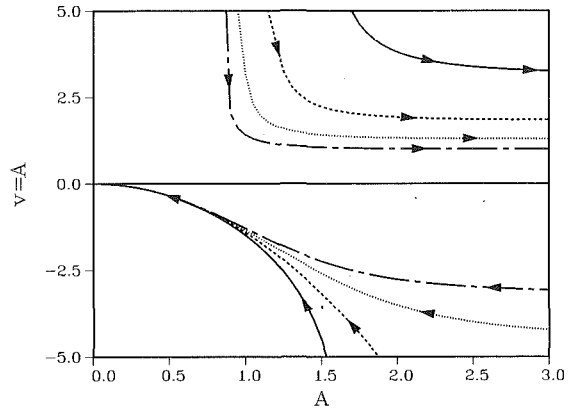

Fig. 6 Phase-plane trajectories for $\gamma = 2$ and $\beta = -1$

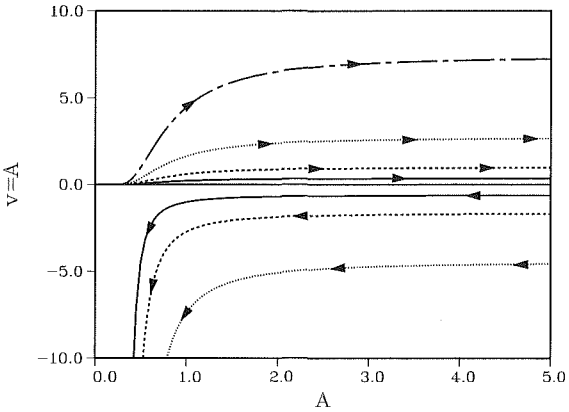

Fig. 7 Phase-plane trajectories for $\gamma = 1$ and $\beta = 1$

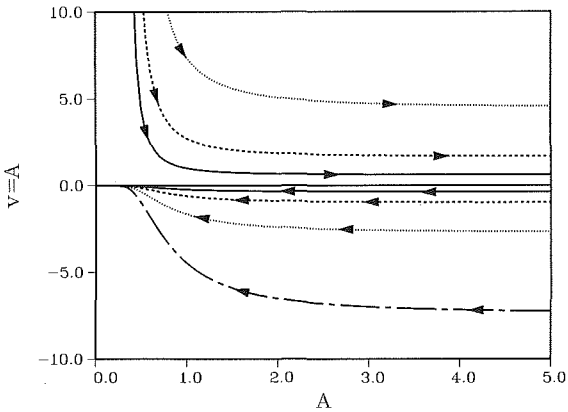

Fig. 8 Phase-plane trajectories for $\gamma = 1$ and $\beta = -1$

The critical points in the phase plane are those that correspond to solutions of (48) that obey $\ddot{A} = \dot{A} = 0$; $A =$ constant. Evidently, such solutions exist and the constant value of $A > 0$ is arbitrary. Thus, critical points of the phase plane lie along the entire positive A-axis for any value of $\gamma > -1$. Because of (45) and (46), the upper half of the phase plane ($v > 0$) corresponds to a tensile edge load, while the lower half plane ($v < 0$) corresponds to a compressive edge load.

Phase plane trajectories are shown in Figs. 3–8. There are three separate cases to consider. The first of these is the case in which $(-1 < \gamma < 1)$. Here, the phase plane trajectories intersect the critical line $v = 0$. Solutions to equation (48) follow the trajectories away from this line if β is positive. For $v = \dot{A} > 0$ (corresponding to a tensile edge load), v tends toward a constant positive value for large time, while A grows without bound. In contrast, if $v < 0$, so that the edge load is compressive, $v \to -\infty$ and A remains bounded as $t \to \infty$.

For $(-1 < \gamma < 1)$ and $\beta < 0$, solutions to (48) move along their phase plane trajectories toward the line $v = 0$, although one can show that $v = 0$ cannot occur in finite time. Thus, as $t \to \infty$ in this case, both A and v approach finite values.

Next, consider the case in which $\gamma > 1$. We suppose first that β is positive. If $v > 0$, then one of either v or A grows without bound, while the other approaches a constant limit. In the lower half plane, however, all trajectories lead to constant values of A while v tends toward negative infinity.

If $\gamma > 1$ and $\beta < 0$, solutions that move on trajectories in the upper half plane have $v \to \infty$ and A approaching a finite limit as $t \to \infty$. In the lower half plane, all solutions approach $v = A = 0$.

When $\gamma = 1$ and $\beta > 0$, solutions that follow trajectories in the upper half plane have velocities that tend toward a constant value as $t \to \infty$, while $A \to \infty$. In the lower half plane, $v \to -\infty$ and A approaches a constant value as $t \to \infty$.

Finally, the behavior of $A(t)$ in the case in which $\gamma = 1$ and $\beta < 0$ is shown in Fig. 8. For large times, velocities tend toward a constant value as A grows without bound (in the upper half of the phase plane) or approach a finite bound (for $v < 0$).

One can show using a continuity argument on (48) that if $\dot{A} \equiv v = 0$ at some instant of time, then $v = 0$ for all time. According to (45) and (46), this corresponds to traction-free edges on the disk. Further, if $v \neq 0$ at some time, then the velocity will never vanish in finite time.

If $\gamma \neq 1$, the first of (70) can be integrated to give the implicit, integral expression for $A(t)$:

$$\pm \int_{A_o}^{A} \left\{ \frac{1}{d \mp \beta \dfrac{1-\gamma}{1+\gamma} a^{-(1+\gamma)}} \right\}^{\frac{1}{1-\gamma}} da = t. \tag{71}$$

Here, A_o is a constant which corresponds to the value of A at time $t = 0$. If the edge load is tensile, so that the radial velocity is positive, then the upper signs in (71) hold; the lower signs correspond to compressive edge loads. If the edges are traction-free, then the velocity is *zero* and (71) must be replaced by $A = A_o$ for all time.

Next, let $\gamma = 1$, so that the phase plane trajectory equations are those appearing in the second of (70). This equation can be integrated to give

$$e^{-d} \int_{A_o}^{A} e^{1/2\beta a^{-2}} da = \pm t. \tag{72}$$

As before, the sign in (72) is chosen according to the direction of the edge load: the upper sign corresponds to tensile edge load, and the lower holds if the loading is compressive. In the tensile case, A becomes unbounded as t grows large. When the loading is compressive, A goes to zero as t tends toward infinity if $\beta > 0$.

The behavior of the edge load $f(t)$ that is required to sustain these motions is found from equations (45) and (46), and the phase plane diagrams. It is seen that $|f(t)| \to 0$ as $t \to \infty$ in all cases, with the exception of those situations in which A approaches a constant limit and $|v|$ tends toward infinity as t gets large. In these cases, one finds that $|f(t)|$ grows without bound.

3 Discussion

The plane-stress assumptions introduced in these analyses are most likely to be valid in the cases in which A grows with

time, so that the edge load is tensile. Compressive edge loads lead to a thickening of the disk, and in this situation, the plane-stress approximations are subject to some question. In the compressive case, one might expect buckling of the disk to occur; this cannot be predicted using the symmetry assumptions of (31). These, in addition to the separated form of $\dot{R}$ that is assumed, also preclude the occurrence of necking in the sheet.

In the tensile edge load case, one might use the solutions obtained here to obtain a time-to-failure of the disk. If one assumes that the disk ruptures when its minimum thickness attains a preassigned critical vale H_*, then the (dimensionless) time t_* to reach H_* is found from equation (71) to be given by

$$\int_{A_o}^{H_*} \left\{ \frac{1}{d-\beta \dfrac{1-\gamma}{1+\gamma}\, a^{-(1+\gamma)}} \right\}^{\frac{1}{1-\gamma}} da = t_*. \tag{73}$$

Acknowledgment

The support of the Army Research Office is gratefully acknowledged.

References

Hutchinson, J. W., Neale, K. W., and Needleman, A., 1978, "Sheet Necking—I. Validity of the Plane Stress Assumptions of the Long-wavelength Approximation," *Mechanics of Sheet Metal Forming*, D. P. Koistinen and N.-M. Wang, eds., Plenum, New York, pp. 111–126.

Needleman, A., and Tvergaard, V., 1977, "Necking of Biaxially Stretched Elastic-Plastic Circular Plates," *Journal of the Mechanics and Physics of Solids*, Vol. 25, pp. 159–183.

Needleman, A., "Necking of Pressurized Spherical Membranes," *Journal of the Mechanics and Physics of Solids*, Vol. 24, pp. 339–359.

Rice, J. R., 1976, "The Localization of Plastic Deformation," *Proceedings of the 14th International Congress of Theoretical and Applied Mechanics*, W. T. Koiter, ed., Vol. 1, pp. 207–220.

Stören, S., and Rice, J. R., 1975, "Localized Necking in Thin Sheets," *Journal of the Mechanics and Physics of Solids*, Vol. 23, pp. 421–441.

Taylor, J. W., Harlow, F. H., and Ainsden, A. A., 1978, "Dynamic Plastic Instabilities in Stretching Plates and Shells," ASME JOURNAL OF APPLIED MECHANICS, Vol. 45, pp. 105–113.